Supplementary Information:

Amorphous FeO_x (x=1, 1.5) coated Cu_3P Nanosheets with Bamboo Leaves-like Morphology induced by Solvent Molecule Selective Adsorption for Highly Active HER Catalysts

Tong Cheng,[a] Xiang Rui,[a] Lishan Peng,[a] Lianqiao Tan,[a] Xianyi Tang,[a] Jianchuan Wang,[a] Li Li,[a*] Qiang Liao [b,c] and Zidong Wei [a*]*

a. National-municipal Joint Engineering Laboratory for Chemical Process Intensification and Reaction, College of Chemistry and Chemical Engineering, Chongqing University, Chongqing, 400044, China.
b. Key Laboratory of Low-grade Energy Utilization Technologies and Systems, Ministry of Education, Chongqing 400030, China.
c. Institute of Engineering Thermophysics, School of Energy and Power Engineering,Chongqing University, Chongqing 400030, China

E-mail: zdwei@cqu.edu.cn (Z. Wei), liliracial@cqu.edu.cn (L. Li)

Experimental Section

Chemicals

Copper foam (thickness of 1.5mm) was purchased from Sai Bo electrochemical materials (China). Ethylene glycol, copper nitrate ($Cu(NO_3)_2$), ferric nitrate ($Fe(NO_3)_3 \cdot 9H_2O$), and urea ($CO(NH_2)_2$) were purchased from Chengdu Kelong Chemical Reagent Factory (China). Ammonium fluoride (NH_4F) and potassium hydroxide (KOH) were purchased from Chongqing Chuandong Chemical Group Co., Ltd.

Characterization

Physical characterization

The composition, surface morphology, and chemical state of the samples were studied with scanning electron microscopy (SEM), powder X-ray diffraction (XRD), X-ray photoelectron spectroscopy (XPS) and transmission electron microscopy (TEM), scanning TEM (STEM) and energy dispersive X-ray spectroscopy (EDX).

Electrochemical measurements

Electrochemical measurements were conducted through a Princeton Applied Research Parstat 4000 potentiostat. Unless mentioned, all electrochemical tests were completed in a standard three-electrode system where Ag/AgCl (3M KCl) was used as the reference electrode and a graphite rod (10 cm in length, 5mm in diameter) was used as the counter electrode. HER tests were conducted in a three-electrode system, the as-prepared samples were used as the work electrode. Prior to collect the polarization curves, 30 cycles CV were conducted between -0.96V and -1.61V (vs. Ag/AgCl) in 1 M KOH. The LSV measurement was conducted between -0.96 V and -1.61 V (vs.Ag/AgCl) under 1 mV/s. EIS test was conducted under 150 mV overpotential with the frequency ranges from 10 kHz to 0.05 Hz. To determine the double layer capacitance, CV scans were conducted at 4 mV/s, 6 mV/s, 8 mV/s, 10 mV/s and 12 mV/s between -0.80 and -0.85 V (vs. Ag/AgCl).

Synthetic procedures

Synthesis of the precursors for g-Cu_3P@Cu, FeO_x-Cu_3P@Cu and g-FeO_x-Cu_3P@Cu

Firstly, the copper foam was sonicated in 3M HCl solution for 20 min and then washed with water and ethanol for several times to remove the surface oxides or pollutants. 3 mmol $Cu(NO_3)_2$, 8 mmol NH_4F (the NH_4F was added to provide F ions, which will be coordinated with metal ions and control the growth speed of precursor on copper foam substrate) and 10 mmol urea (the urea was added as the precipitator, and the decomposition of urea at high temperature can provide NH_3 which will help the deposition of M^{x+}) were dissolved in 30 ml solution containing 5 ml ethylene glycol and 25 ml deionized water, then stirred for 20 min (pH= ~ 2). The as-obtained solution was then added into a 50 mL Teflon-lined stainless steel autoclave, followed by the clean copper foam immersing in the solution, then the autoclave was sealed and heated up to 120 ℃ for 12h. The resultant was rinsed with deionized water for several times, dried in vacuum at 60 ℃ for 8 h, then the precursor of g-Cu_3P@Cu was obtained. The precursor of FeO_x- Cu_3P@Cu was synthesized in the same condition, except for a different ratio of water/ethylene glycol (30/0) and an addition of 3 mmol $Fe(NO_3)_3$. The precursors of g-FeO_x-Cu_3P@Cu was synthesized in the same condition, except for an addition of 3 mmol $Fe(NO_3)_3$.

Synthesis of g-Cu_3P@Cu, FeO_x-Cu_3P@Cu and g-FeO_x-Cu_3P@Cu

The NaH_2PO_2 was put upstream in the tube furnace and the precursors of g-Cu_3P@Cu, FeO_x-Cu_3P@Cu and g-FeO_x-Cu_3P@Cu were put downstream, then heated up to 400 ℃ with a stable rate of 5 ℃/ min and held for 90 min in N_2 atmosphere. The as-obtained samples were g-Cu_3P@Cu, FeO_x-Cu_3P@Cu and g-FeO_x-Cu_3P@Cu respectively. The copper foam was phosphorylated under 400℃ for 90 min in N_2 atmosphere as the control sample.

Synthesis of Pt/C@Cu

20 wt% Pt/C@Cu was synthesized by mixing 4 mg commercial Pt/C with 40 μL 5

wt% Nafion, 160 μL ethanol and 800 μL H_2O to form a homogeneous ink. Then 500 μL of the homogeneous ink was loaded on the copper foam (1 cm×1 cm×1.5 mm) as the Pt/C@Cu (2 mg cm^{-2}).

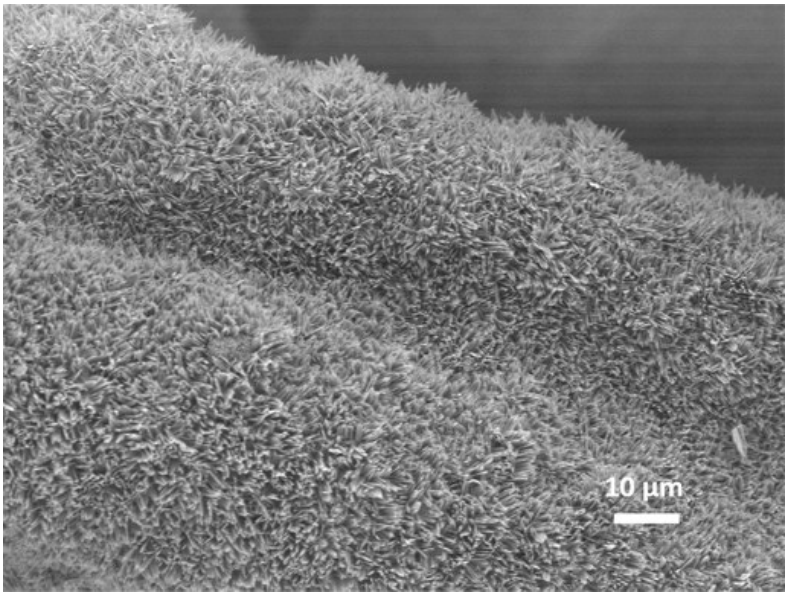

Figure S1. SEM images of bamboo leaves like hydrothermal precursor under 10 µm scale

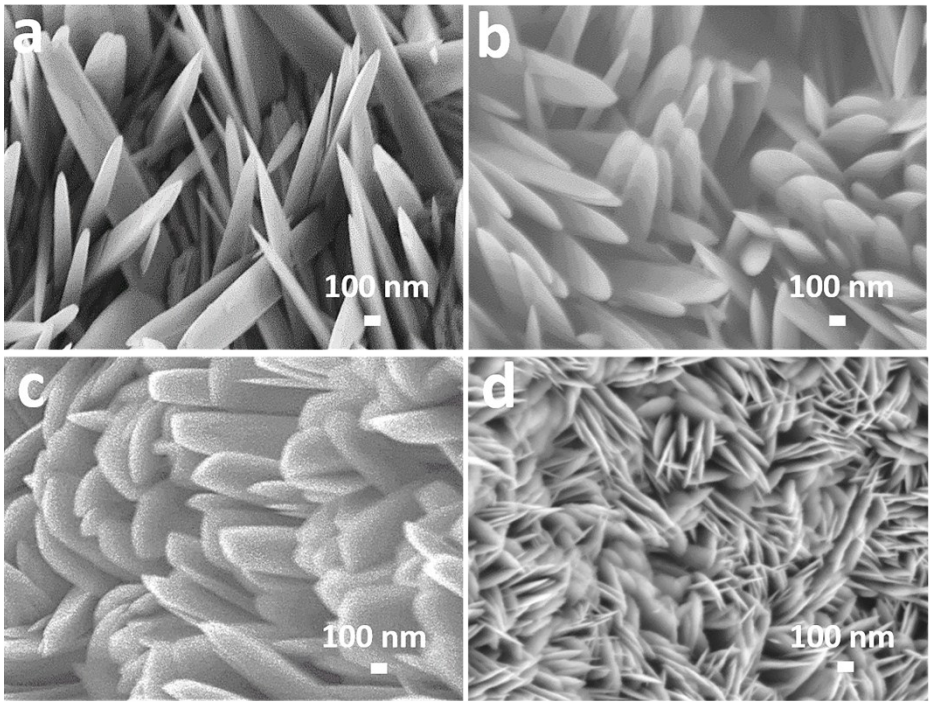

Figure S2. SEM images of hydrothermal precursor formed in a) 5 ml ethylene glycol+25 ml H_2O; b) 10ml ethylene glycol+20 ml H_2O; c) 15 ml ethylene glycol+15 ml H_2O and d) 20ml ethylene glycol+10 ml H_2O.

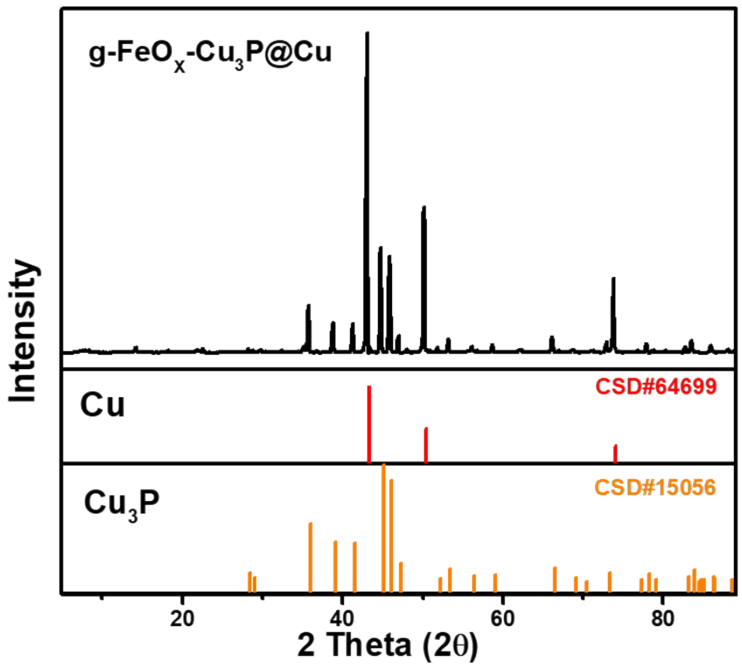

Figure S3. XRD patterns of g-FeO_x-Cu_3P@Cu

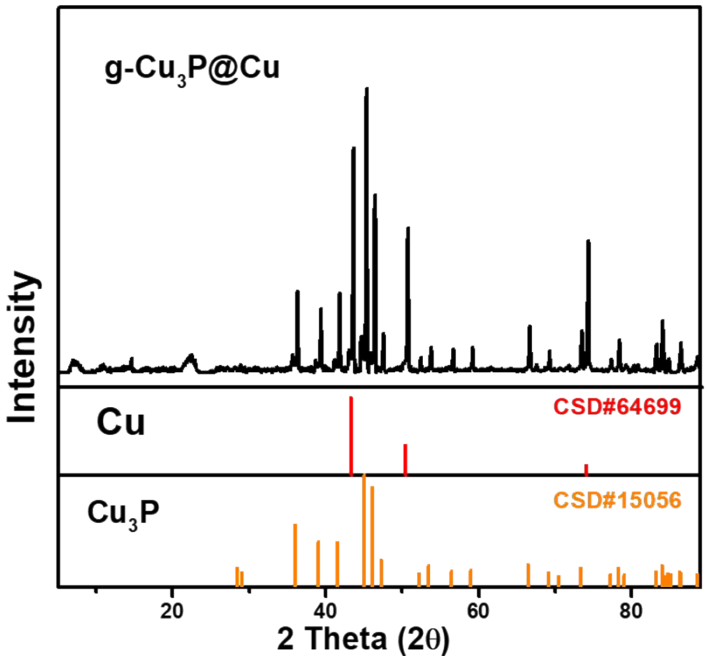

Figure S4. XRD patterns of g-Cu_3P@Cu

The peaks around 36.0°, 39.5°, 41.5°, 45.1°, 46.2°, 47.2°, 53.5°, 59.0°, 66.5°, 73.4° and 78.3° correspond to the (112), (202), (211), (300), (113), (212), (104), (222), (214), (322) and (314) facets of Cu_3P (CSD#15056), respectively, demonstrating the formation of Cu_3P.

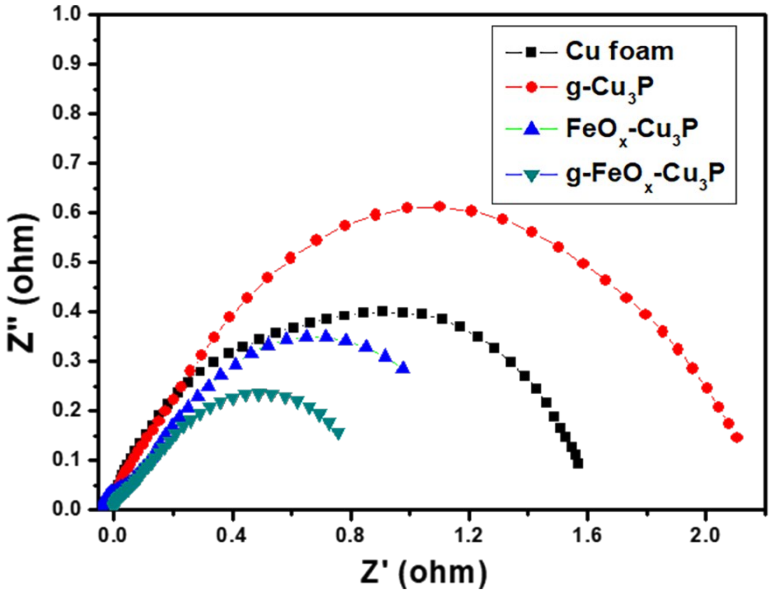

Figure S5. Nyquist plots measured at a voltage of −0.15 V (vs RHE) over the frequency range 100 kHz to 0.05 Hz in 1.0 M KOH of Cu foam (Phosphorylated), g-Cu_3P, FeO_x-Cu_3P, g-FeO_x-Cu_3P.

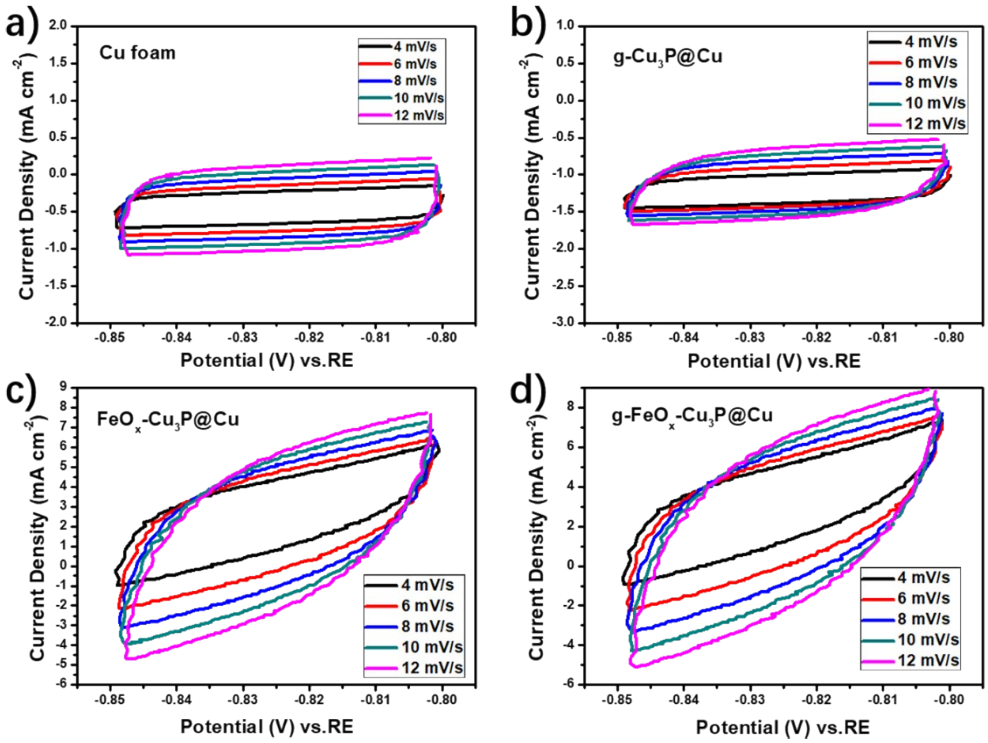

Figure S6. CVs of different samples a) Cu foam (Phosphorylated) b) g-Cu_3P c) FeO_x-Cu_3P and d) g-FeO_x-Cu_3P with various scan rates (4-12 mV/s) in the region of 0.8 to 0.85 V vs. RE.

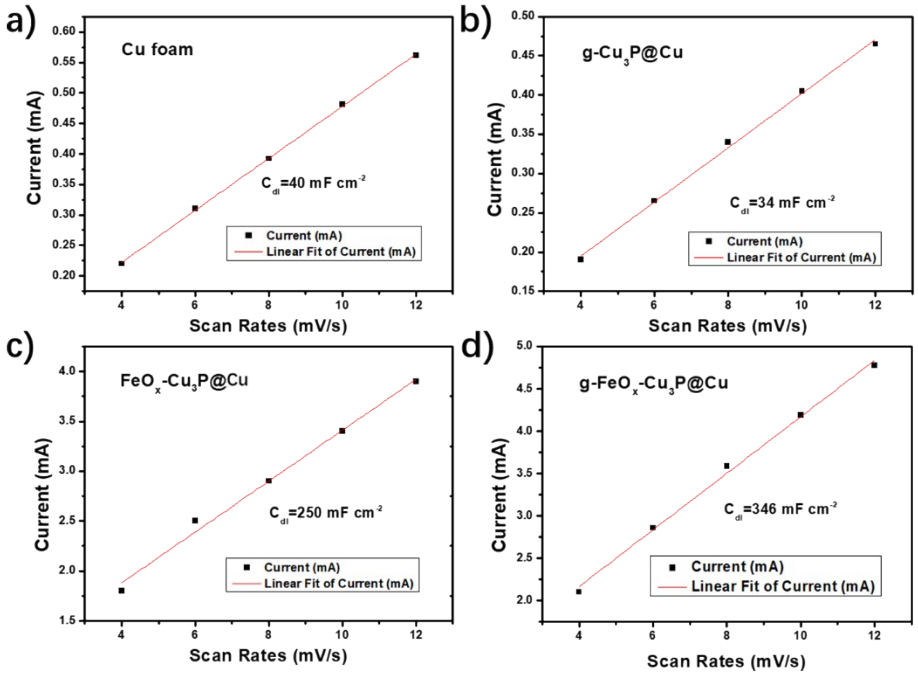

Figure S7. Estimation of C_{dl} of a) Cu foam (Phosphorylated), b) g-Cu_3P@Cu, c) FeO_x-Cu_3P@Cu, d) g-FeO_x-Cu_3P@Cu by plotting the current density variation ($\Delta j = (ja - jc)/2$) at 0.83V vs RE and fitting.

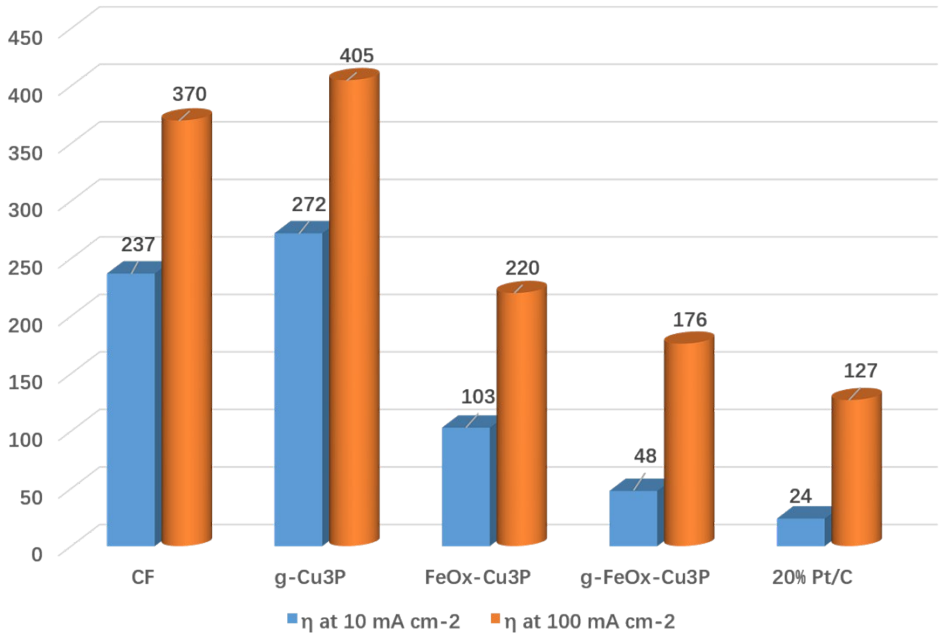

Chart S1. Overpotential for Cu foam (Phosphorylated), g-Cu_3P@Cu, FeO_x-Cu_3P@Cu, g-FeO_x-Cu_3P@Cu and 20% Pt/C at 10/100 mA cm^{-2}

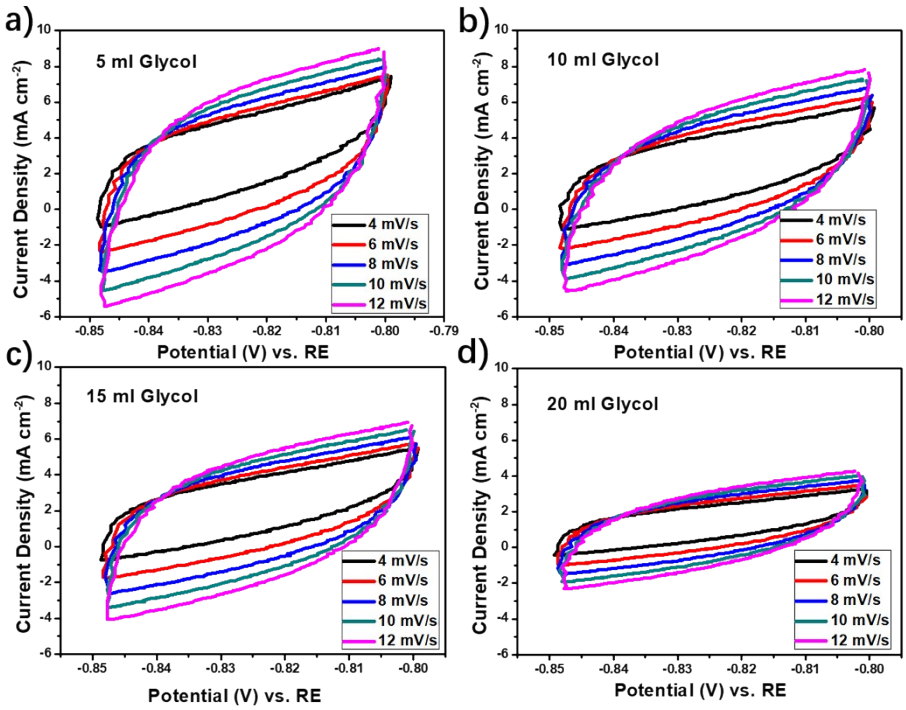

Figure S8. CVs of different samples fabricated in solvent that contains a) 5 ml ethylene glycol b) 10 ml ethylene glycol c) 15ml ethylene glycol and d) 20 ml ethylene glycol with various scan rates (4-12 mV/s) in the region of 0.8 to 0.85 V vs. RE.

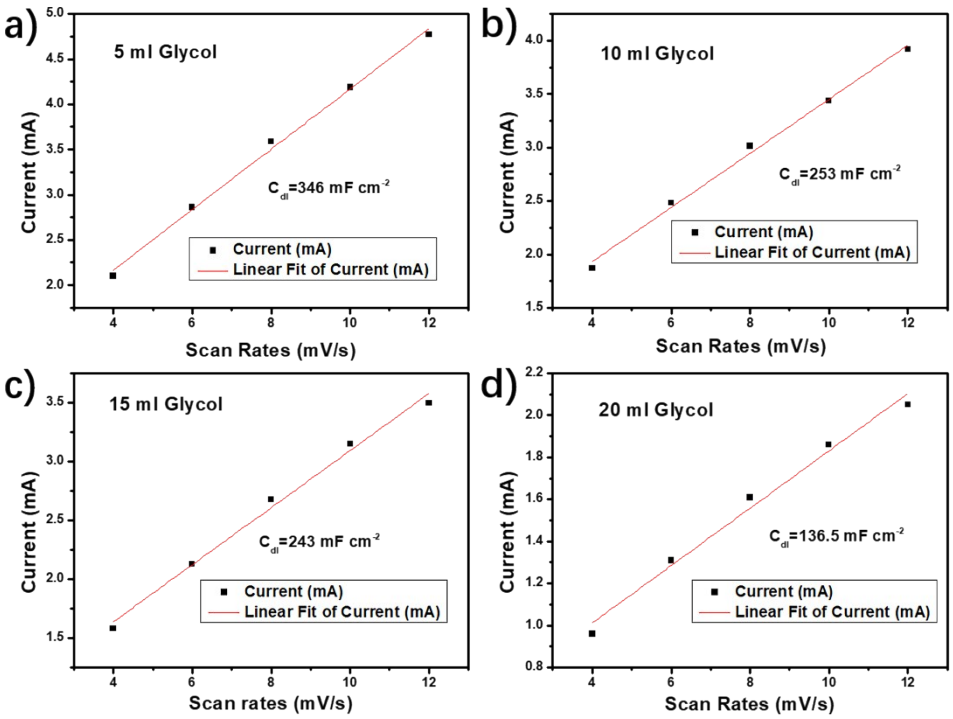

Figure S9. Estimation of Cdl of different samples fabricated in solvent that contains a) 5 ml ethylene glycol b) 10 ml ethylene glycol c) 15ml ethylene glycol and d) 20 ml ethylene glycol by plotting the current density variation ($\Delta j = (ja–jc)/2$) at 0.83V vs RE and fitting.

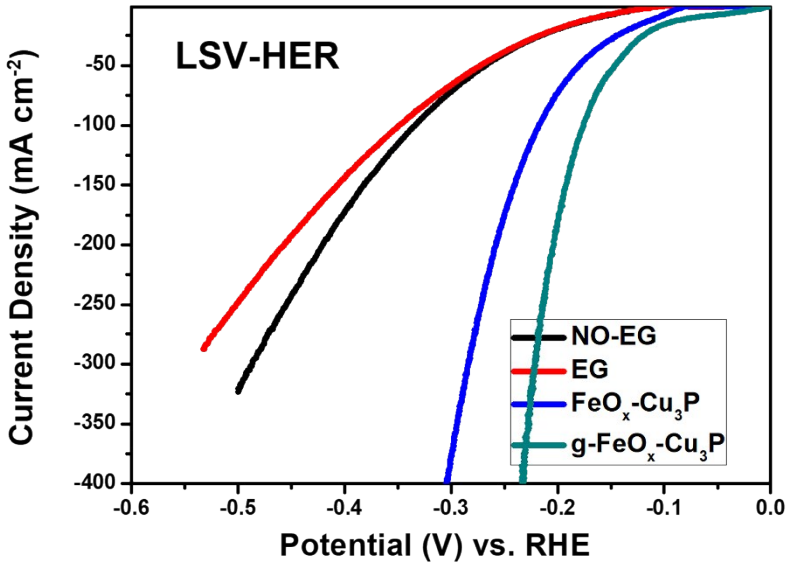

Figure S10. LSV curves of hydrothermal precursor fabricated without ethylene glycol (called NO-EG), hydrothermal precursor fabricated with ethylene glycol (called EG), FeO_x-Cu_3P@Cu and g-FeO_x-Cu_3P@Cu in 1 M KOH with a scan rate of 1mV s^{-1}.

Before the phosphidation process, the precursors of FeO_x-Cu_3P@Cu and g-FeO_x-Cu_3P@Cu showed poor HER activity (167mV and 169 mV at 10 mA cm^{-2}, respectively). However, after the phosphidation, FeO_x-Cu_3P@Cu and g-FeO_x-Cu_3P@Cu showed large improvement (103 mV and 48 mV at 10 mA cm^{-2}, respectively) comparing to their precursors respectively.

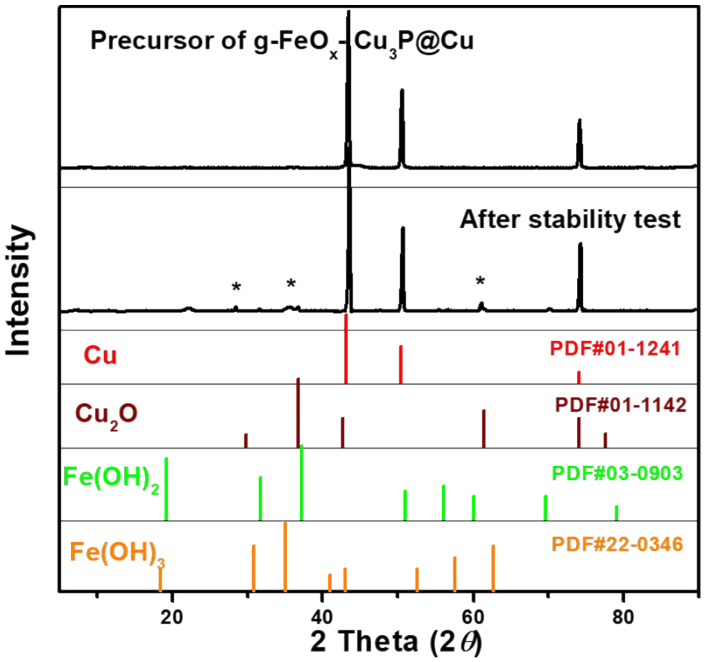

Figure S11. XRD patterns of g-FeO_x-Cu_3P@Cu precursor before and after the stability test.

From the XRD results, the sample of hydrothermal precursor only exhibited the peaks of copper which suggested precursors is amorphous. After the stability tests, some new peaks appeared. It could be ascribed to the Cu_2O generated during the stability tests. There were one or two peaks matched with the standard PDF cards of $Fe(OH)_2$ and $Fe(OH)_3$, which indicated a little FeO_x in the precursor may have changed to crystalline $Fe(OH)_x$.

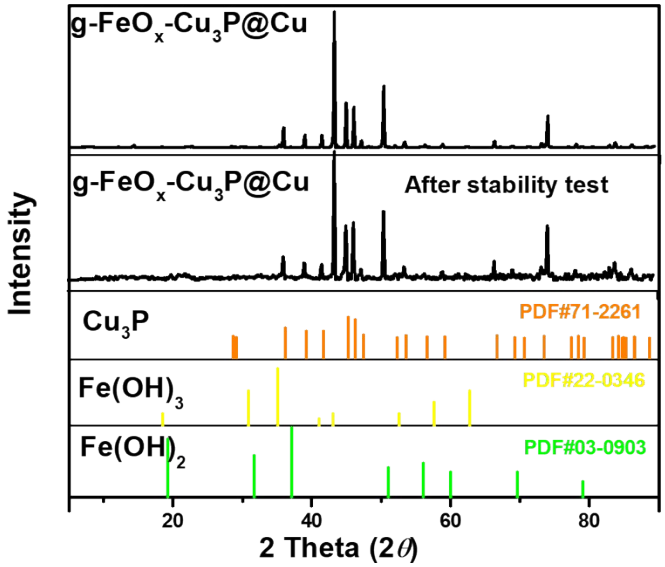

Figure S12. XRD patterns of g-FeO_x-Cu_3P@Cu before and after the stability test.

The XDR patterns of g-FeO_x-Cu_3P@Cu after stability test still exhibited the peaks of Cu_3P .After the stability tests, some new peaks appeared. It could be ascribed to the Cu_2O generated during the stability tests. There were one or two peaks matched with the standard PDF cards of $Fe(OH)_2$ and $Fe(OH)_3$, which indicated a little FeO_x in the precursor may have changed to crystalline $Fe(OH)_x$.

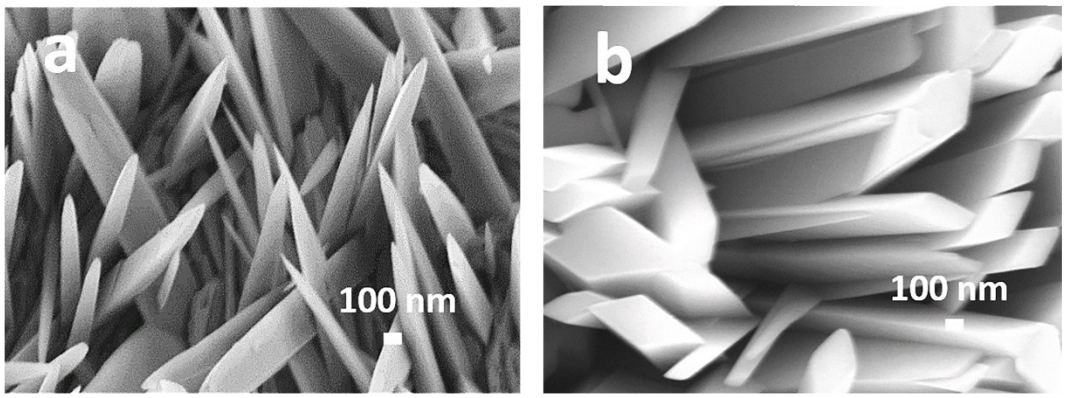

Figure S13. a) SEM images of hydrothermal precursor fabricated with ethylene glycol; b) hydrothermal precursor fabricated with ethylene glycol after stability tests.

The morphology of the hydrothermal precursor changed after stability tests, which could be attributed to the reduction of Fe^{3+} or Cu^{2+} on the surface and the recrystallization of the precursor.

Table S1. Overpotential of Cu foam, g-Cu_3P@Cu, FeOx-Cu3P@Cu, g-FeOx-Cu3P@Cu and 20% Pt/C at 10 mA cm^{-2}

Samples	**Overpotential at 10mA cm^{-2}**
Cu foam	237 mV
g-Cu_3P	272 mV
FeO_x-Cu_3P	103 mV
g-FeO_x-Cu_3P	48 mV
20% Pt/C	24 mV

Table S2. Overpotential of Cu foam, g-Cu_3P@Cu, FeO_x-Cu_3P@Cu, g-FeO_x-Cu_3P@Cu and 20% Pt/C at 100 mA cm^{-2}

Samples	**Overpotential at 100 mA cm^{-2}**
Cu foam	370 mV
g-Cu_3P	405 mV
FeO_x-Cu_3P	220 mV
g-FeO_x-Cu_3P	176 mV
20% Pt/C	127 mV

Table S3. ECSA of different samples fabricated in solvent that contains 5 ml ethylene glycol, 10 ml ethylene glycol, 15ml ethylene glycol and 20 ml ethylene glycol

Volume of Ethylene glycol	**ECSA (mF cm^{-2})**
0 ml	250
5 ml	346
10 ml	253
15 ml	243
20 ml	136

Table S4. Summary of the HER performances of different materials reported recently.

Electrocatalysts	Electrolyte	Overpotential (mV@10 mA cm^{-2})	Reference
20% Pt/C	1 M KOH	24	-
g-FeO_x-Cu_3P@Cu	1 M KOH	48	-
Cu NDs/Ni_3S_2 NTs-CFs	1 M KOH	128	J. Am. Chem. Soc. 2018, 140, 610-617.
Cu_3P@NPPC	0.5 M H_2SO_4	89	Adv. Mater. 2018, 30, 1703711
Cu_3P/CF	1 M KOH	210@20 mA cm^{-2}	J. Phys. Chem. C 2017, 121, 25875-25881
FeP Nanoparticles	0.5 M H_2SO_4	154	ACS Catal. 2016, 6, 5441-5448
carbon-shell-coated FeP NPs	0.5 M H_2SO_4	71	J. Am. Chem. Soc. 2017, 139, 6669-6674
Fe-CoP UNSs/NF	1 M KOH	67	J. Mater. Chem. A, 2019, 7, 20658–20666
FeS|P/CNT	0.5 M H_2SO_4	79	ACS Catal. 2017, 7, 4026−4032
CoP–Mo_2C on N-doped carbon	1 M KOH	94	ChemSusChem, 2018, 11, 3956–3964.